Structural Transitions of Solvent-Free Oligomer-Grafted Nanoparticles

Alexandros Chremos and Athanassios Z. Panagiotopoulos*

Department of Chemical and Biological Engineering, Princeton University, Princeton, New Jersey 08540, USA

(Received 1 June 2011; published 1 September 2011)

Novel structural transitions of solvent-free oligomer-grafted nanoparticles are investigated by using molecular dynamics simulations of a coarse-grained bead-spring model. Variations in core size and grafting density lead to self-assembly of the nanoparticles into a variety of distinct structures. At the boundaries between different structures, the nanoparticle systems undergo thermoreversible transitions. This structural behavior, which has not been previously reported, deviates significantly from that of simple liquids. The reversible nature of these transitions in solvent-free conditions offers new ways to control self-assembly of nanoparticles at experimentally accessible conditions.

DOI: 10.1103/PhysRevLett.107.105503 PACS numbers: 61.46.Df, 61.20.−p, 61.25.−f

In the past decade, considerable effort has gone into efficiently creating microstructures by tuning the geometrical or chemical characteristics of self-organizing molecular blocks, because of potential applications in photonics and electronics [1], energy storage [2], chemical and biological storage [3], and drug delivery [4]. There have been several experimental demonstrations of controlled self-assembly using oligomer-grafted nanoparticles [5–7]. In addition, numerous simulation studies offered insights into the parameters controlling the behavior of grafted nanoparticles [8–14]. These studies have mainly focused on self-assembly in solution. Grafted nanoparticles have similarities with supramolecular polymers [15], which are held together by highly directional noncovalent interactions. The reversible nature of supramolecular polymers makes them attractive as molecular building blocks for the design of ''smart'' polymeric materials. However, these polymers work well in solution but not in meltlike conditions. Nanoparticle organic hybrid materials [16–18] are novel core-shell particle systems, in which each particle consists of a hard (inorganic) core and a soft (organic) oligomer corona. Nanoparticle organic hybrid materials in solvent-free conditions can still be liquids, and so the coronas effectively become the solvent. This creates a unique physical environment.

Despite the existence of a considerable body of literature on chain-grafted nanoparticles in solution or within a polymeric matrix, little is known about the structural behavior of such systems in the absence of solvent. Star polymer melts are a limited case of solvent-free grafted nanoparticles and can display liquidlike behavior by tuning the number and length of the grafted chains [19]. The core size in star polymers is significantly smaller than the contour length of the chains and is frequently neglected, which is not the case for grafted nanoparticles. The primary focus of this Letter is to gain an understanding of the structural behavior of solvent-free oligomer-grafted nanoparticles when the core size becomes significant. In particular, we use molecular dynamics simulations to investigate the structures formed by varying the nanoparticle core size and number of tethered chains while keeping the chain length fixed. We illustrate that a rich variety of structures is obtained. At the boundaries between different types of structures, the nanoparticles undergo thermoreversible transitions between the two types of neighboring structures. These are, of course, not true phase transitions, as they are not associated with discontinuities in any thermodynamics properties.

Our model system consists of $N = 400$ nanoparticles, where each nanoparticle is represented as a spherical core with f attached oligomer chains. The chains are composed of N_m spherical beads of size σ connected to form a chain. By varying the geometric characteristics of the model, its molecular architecture can resemble a star polymer or a polymer-coated colloid. In particular, we investigate the effects of nanoparticle core size D_c and number of grafted chains f while keeping the number of beads of each grafted chain at $N_m = 10$. Bonds are described by a harmonic potential $V_{\mathrm{H}}(r) = k(r - l_0)^2$, where r is the bead-bead separation, l_0 is the natural length of the spring equal to the diameter of polymer bead, $l_0 = 1\sigma$, and k is a spring constant: $k = 5000\varepsilon/\sigma^2$. The polymer beads attached to a core particle have fixed coordinates with respect to the nanoparticle. The size of the nanoparticle, D_c, varies from 0.5σ to 8σ. The mass of a particle scales linearly with volume, so that $m_b = m$ and $m_c = mD_c^3/\sigma^3$ for the mass of the polymer bead and core, respectively. The polymer-bead interactions are described by a Lennard-Jones potential with cutoff distance $r_{\mathrm{cut}} = 2.5\sigma$. For the core-core and core-polymer interactions, we use the purely repulsive Weeks-Chandler-Andersen potential [20], modified to take into account the difference in particle size [21]. Simulations were performed in cubic boxes; periodic boundary conditions and the minimum-image convention were applied in all three spatial directions. The simulations were performed by using the Large-Scale Atomic/Molecular Massively Parallel Simulator [22], which takes advantage of neighbor lists and a special-purpose communication algorithm to

maintain good performance when the size ratio of interaction centers becomes large [23].

The nanoparticle volume fraction can be altered by changing the grafting density, chain length, and density or temperature. A wide range of polymer-bead densities in free space, $\rho_b = NfN_m/(L^3 - N\pi D_c^3/6)$, were explored (from $\rho_b = 0.55$ to 0.85), at which the system was equilibrated in the NVT ensemble at a temperature that corresponds to zero pressure, thus matching the common experimentally used atmospheric conditions. After equilibration, production runs of 2×10^7 steps each were performed in the NVE ensemble. A typical run required 10 wall-clock days on 8 cores of Intel 2.83 GHz "Nehalem" processors.

The key structural changes observed are illustrated in Fig. 1. The core-core radial distribution function $g_{cc}(r)$ for two systems with the same core size $D_c = 2\sigma$, but different numbers of grafted chains, $f = 4$ and $f = 32$, is shown in Fig. 1(a). For low density ($\rho_b = 0.55$) both systems display liquidlike behavior, though in the case of $f = 4$ the system is much less structured than for $f = 32$. Nevertheless, nanoparticle aggregation is prevented due to the steric "protection" that the grafted chains offer. For higher densities, nanoparticles with $f = 32$ continue to have liquidlike behavior similar to that at lower densities. However, the $f = 32$ does not follow typical simple-liquid behavior; as temperature increases, the peaks in $g_{cc}(r)$ not only shift to larger distances but also become higher (more structured). Density decreases with increasing T^*, so more "free space" is available to the nanoparticles at the higher temperatures. This additional empty space can be considered as an added "phantom solvent" that reduces the net monomer-monomer attraction. Even though we did not attempt this here, our model could also be generalized to systems with an explicit solvent. In the present work, increasing T^* is equivalent to creating a better solvent condition for the oligomers and makes the monomer-monomer excluded volume more important. Therefore, the shift in the peaks of g_{cc} is more observable in simulations as the corona expands and gives rise to more substantial steric effect among the particles at higher T^*. This is consistent with observations in star polymer solutions [24,25] and sterically stabilized colloidal suspensions [26]. On the other hand, in the radial distribution function of $f = 4$, a sharp peak is manifested at $r/D_c = 1$, suggesting aggregation. The peak emerges despite the fact that the core-core interactions are purely repulsive. Moreover, when two nanoparticles come together, they push the surrounding grafted chains to the side, which in turn prevent other nanoparticles joining the side of the aggregate. This leads to a formation of string or sheetlike structures. These structures have the tendency to form a percolating network, which is a characteristic of a gel [27]. The transition from one structure to another is reversible, because there is no chemical bonding and so the structural changes can be triggered by changing temperature. The formation of anisotropic structures from isotropic particles (oligomer-grafted nanoparticles in polymer matrix) has been reported for oligomer-grafted nanoparticles in polymer matrix [5]. The issue of optimum grafting density for dispersing grafted nanoparticles in a polymer matrix is also discussed in Ref. [28]. The case of $f = 32$, for which the nanoparticles have liquidlike behavior and display more structure within the density (temperature) range explored, will be described as a star liquid. For $f = 4$ the structural behavior indicates that the system behaves as a thermoreversible anisotropic aggregation (G-1), since by varying the density (temperature) the nanoparticles form stringlike structures at high density (low temperature), while for low density (high temperature) the nanoparticles are well dispersed.

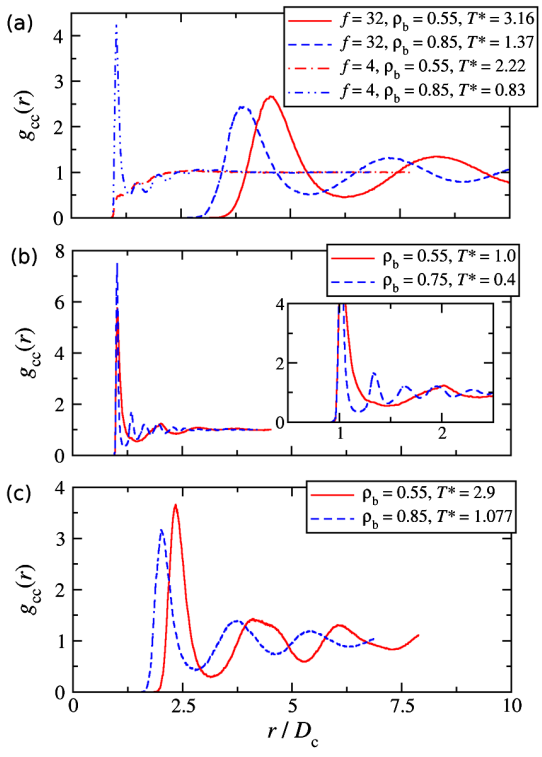

FIG. 1 (color online). Radial distribution functions at different densities and temperatures: (a) $D_c = 2\sigma$, $f = 4$ and 32; (b) $D_c = 3\sigma$, $f = 2$; (c) $D_c = 5\sigma$, $f = 64$.

For systems with lower grafting density, such as $f = 2$ and $D_c = 3\sigma$ as seen in Fig. 1(b), a percolating network forms at lower densities. This is reflected on the radial distribution function with the location of the second peak being at $r/D_c = 2$. However, at higher densities $\rho_b = 0.75$, the stringlike structures collapse with the formation of larger isotropic colloidal clusters leading to the emergence of structural characteristics between the first and second peaks of g_{cc} at lower densities. The above structural transition is identified as thermoreversible isotropic aggregation (G-2). The defining difference between

G-2 and G-1 structures is that the grafting density is low enough to prevent nanoparticles from aggregating even at low densities (high temperatures).

Increasing the number of grafted chains on a nanoparticle not only protects the nanoparticles from aggregation but also increases the effective size of a particle. In star polymers, the number of grafted chains tunes the softness and acts as a bridge between polymers and colloids [29]. We observe the same trend for the nanoparticles, but this has another interesting effect. For $f = 64$, although at high density ($\rho_b = 0.85$) the system has liquidlike characteristics, at lower density solidlike characteristics manifest themselves; see Fig. 1(c). This is in contrast to simple-liquid behavior where rigidlike characteristics emerge with increasing density (lowering temperature). The key difference is the subtle way the corona affects the effective size of the particles. An increase in temperature would increase the interparticle distance, which is observed at the shift of the radial distribution function's peaks; see Fig. 1(c). But an increase on the interparticle spacing would cause the oligomers to stretch outwards in an attempt to fill the surrounding space, while the coronas of neighboring nanoparticles continue to overlap with each other. However, even though interparticle spacing has increased, the particles' effective size becomes larger, because neighboring overlapping coronas experience entropic penalties due to the increase of temperature and the chain stretching. A similar effect has been observed in concentrated star polymer solutions [24,25]. This interpretation is also reflected in the core mean-square displacement (MSD); see Fig. 2. For lower density the nanoparticles do not reach a diffusive regime within the accessible simulation times, but for higher density the cores reach it. Moreover, at $t \approx 2.8 \times 10^4 \tau$ the MSD for $\rho_b = 0.85$ has reached the MSD of $\rho_b = 0.55$, signifying the importance of the corona's thermal expansion. The MSD for lower grafting density, $f = 16$, shows a diffusive behavior for lower density but not for higher density, because nanoparticles aggregate and thus the nanoparticles display a subdiffusive behavior within the accessible simulation times; see Fig. 2. A system is identified as glass if it is nonergodic; however, for $f = 64$, it was not computationally feasible to determine that. Nevertheless, we would consider that $f = 64$ has a glassy behavior at higher T^*, because the second peak of $g_{cc}(r)$ becomes wider with a tendency to split [Fig. 1(c)] and has a nondiffusive behavior (Fig. 2). Hence, $f = 64$ deviates from star liquids because the thermal expansion of the corona triggers a vitrification at higher temperatures; such structural behavior will be identified as a glass-forming star liquid.

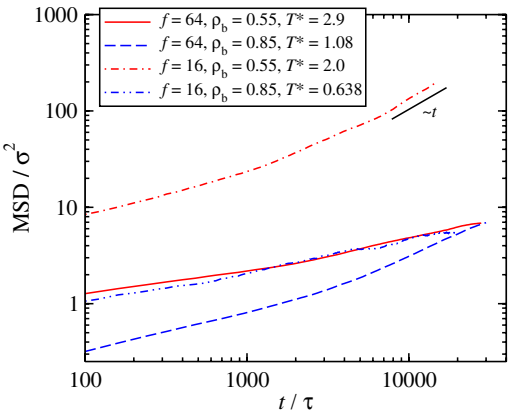

FIG. 2 (color online). Mean-square displacement of solvent-free oligomer-grafted nanoparticles with $D_c = 5\sigma$.

To organize the structural behavior of the model systems, we construct structural maps for a fixed number of grafted chains or core size. Figure 3 (top) shows the structures observed as a function of temperature and core size for $f = 4$. The particles have a liquidlike structure when the core size is small, but as the core size increases the corona cannot prevent aggregation [see Fig. 1(a) for the $g_{cc}(r)$ with $f = 4$ and $D_c = 2\sigma$]. Figure 3 (bottom) shows the effects of f and temperature for $D_c = 5\sigma$. Another important insight is obtained when considering packing effects at the same temperature. From Fig. 3, we can deduce that the particles can pack more efficiently (higher values of ρ_b) by decreasing the core size or increasing the grafting density. Increasing T^* not only reduces the density (at constant pressure) but also enhances excluded volume effects. As discussed above, for a star liquid increasing T^* enhances structure, and for highly packed systems (as observed for $f = 64$) the coronal thermal expansion triggers a vitrification. Although it is difficult in practice to synthesize monodisperse particles, the structural maps may act as a reference point for future experimental studies.

Figure 4 provides a structural map as a function of core size and number of grafted chains, implicitly

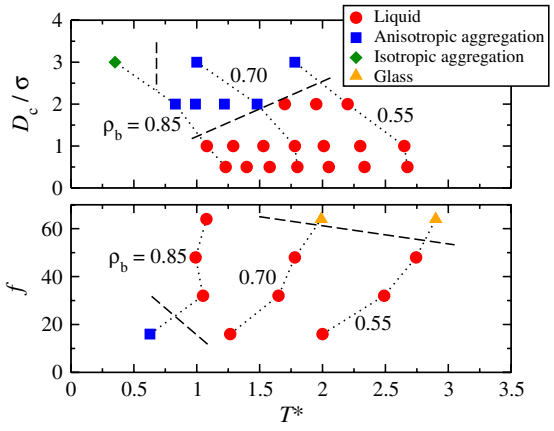

FIG. 3 (color online). Top: Structural behavior of nanoparticles with $f = 4$. Bottom: Structural behavior of nanoparticles with $D_c = 5\sigma$. The dashed lines outline the different morphologies, and the dotted lines correspond to systems with the same polymer-bead density ρ_b.

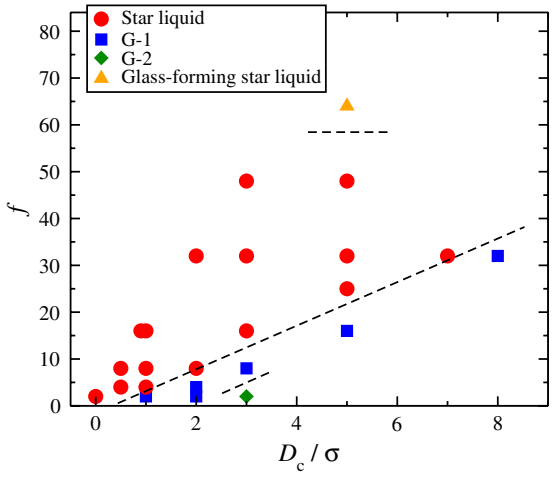

FIG. 4 (color online). Structural behavior map of solvent-free oligomer-grafted nanoparticles with fixed chain length $N_m = 10$. The dashed lines are approximate boundaries between different behaviors.

incorporating the temperature effects shown in Fig. 3. For small nanoparticle sizes, star liquid behavior is expected. But for larger nanoparticles, the number of grafted oligomers determine the structural behavior. For example, for $D_c = 5\sigma$ and for a small number of grafted oligomers, e.g., $f = 16$, the system enters into thermoreversible aggregation. For higher f, the corona is stiff enough to protect the core from aggregation, and thus a star liquid is observed. For $f > 48$ the corona becomes significantly stiffer, resulting in more structural characteristics, and at $f = 64$ the system becomes a glass-forming star liquid.

In summary, chain-grafted nanoparticles offer flexibility in the design of new smart materials due to their hybrid character and their ability to exist as liquids in the absence of solvent. These systems undergo structural transitions due to the subtle interplay of core size and grafting density. For a sufficiently large core and high grafting density, they resemble star polymers, where the thermal expansion of the corona traps the nanoparticles and a glassy behavior is observed. On the other hand, for a low enough grafting density, the corona cannot prevent neighboring nanoparticles from aggregating. Akcora *et al.* [5] have reported the formation of anisotropic (stringlike) structures, with isotropic polymer-grafted nanoparticles in a polymer matrix. The current study expands the findings of Ref. [5] to systems without an external solvent medium. The structural maps obtained in this study provide insights on how the geometric characteristics of the particles can be tuned to achieve experimentally desired structural behavior. These systems can be considered to be experimentally realizable versions of a class of models with short-range attractions and longer-range repulsions (e.g., [30]). Experimental synthesis and characterization of appropriate nanoparticle organic hybrid material systems can be used in the future to validate the predictions of the present work.

The authors thank F. Escobedo for suggesting the simulation model used in this work and D. Koch, H.-Y. Yu, and S. Kumar for helpful discussions. This Letter is based on work supported by Grant No. KUS-C1-018-02 made by King Abdullah University of Science and Technology and by Grant No. CBET-1033155 from the U.S. National Science Foundation.

*azp@princeton.edu

[1] O. D. Velev, P. M. Tessier, A. M. Lenhoff, and E. W. Kaler, Nature (London) **401**, 548 (1999).
[2] A. S. Arico, P. Bruce, B. Scrosati, J. M. Tarascon, and W. V. Schalkwijk, Nature Mater. **4**, 366 (2005).
[3] G. F. Zheng, F. Patolsky, Y. Cui, W. U. Wang, and C. M. Lieber, Nat. Biotechnol. **23**, 1294 (2005).
[4] G. Han, P. Ghosh, and V. M. Rotello, Nanomedicine **2**, 113 (2007).
[5] P. Akcora *et al.*, Nature Mater. **8**, 354 (2009).
[6] Z. L. Zhang, M. A. Horsch, M. H. Lamm, and S. C. Glotzer, Nano Lett. **3**, 1341 (2003).
[7] D. Nykypanchuk, M. M. Maye, D. van der Lelie, and O. Gang, Nature (London) **451**, 549 (2008).
[8] A. Jayaraman and K. S. Schweiser, J. Chem. Phys. **128**, 164904 (2008).
[9] A. Jayaraman and K. S. Schweiser, Langmuir **24**, 11 119 (2008).
[10] X. Zhang, Z. L. Zhang, and S. C. Glotzer, Nanotechnology **18**, 115706 (2007).
[11] M. A. Horsch, Z. Zhang, and S. C. Glotzer, Nano Lett. **6**, 2406 (2006).
[12] M. R. Wilson, A. B. Thomas, M. Dennison, and A. J. Masters, Soft Matter **5**, 363 (2009).
[13] E. R. Chan, L. C. Ho, and S. C. Glotzer, J. Chem. Phys. **125**, 064905 (2006).
[14] C. R. Iacovella, A. S. Keys, M. A. Horsch, and S. C. Glotzer, Phys. Rev. E **75**, 040801 (2007).
[15] L. Brunsveld, B. J. B. Folmer, E. W. Meijer, and R. P. Sijbesma, Chem. Rev. **101**, 4071 (2001).
[16] H.-Y. Yu and D. Koch, Langmuir **26**, 16 801 (2010).
[17] J. L. Nugent, S. S. Moganty, and L. A. Archer, Adv. Mater. **22**, 3677 (2010).
[18] A. B. Bourlinos, R. Herrera, N. Chalkias, D. D. Jiang, Q. Zhang, L. A. Archer, and E. P. Giannelis, Adv. Mater. **17**, 234 (2005).
[19] T. Pakula, D. Vlassopoulos, G. Fytas, and J. Roovers, Macromolecules **31**, 8931 (1998).
[20] J. D. Weeks, D. Chandler, and H. C. Andersen, J. Chem. Phys. **54**, 5237 (1971).
[21] J. S. Smith, D. Bedrov, and G. D. Smith, Compos. Sci. Technol. **63**, 1599 (2003).
[22] S. J. Plimpton, J. Comput. Phys. **117**, 1 (1995).
[23] P. J. in't Veld, S. J. Plimpton, and G. S. Grest, Comput. Phys. Commun. **179**, 320 (2008).
[24] M. Kapnistos, D. Vlassopoulos, G. Fytas, K. Mortensen, G. Fleischer, and J. Roovers, Phys. Rev. Lett. **85**, 4072 (2000).
[25] A. N. Rissanou, D. Vlassopoulos, and I. A. Bitsanis, Phys. Rev. E **71**, 011402 (2005).

[26] U. Genz, B. D'Aguanno, J. Mewis, and R. Klein, Langmuir **10**, 2206 (1994).
[27] C. Daniel, C. Dammer, and J.-M. Guenet, Polymer **35**, 4243 (1994).
[28] D. L. Green and J. Mewis, Langmuir **22**, 9546 (2006).
[29] C. N. Likos, H. Löwen, M. Watzlawek, B. Abbas, O. Jucknischke, J. Allgaier, and D. Richter, Phys. Rev. Lett. **80**, 4450 (1998).
[30] S. Mossa, F. Sciortino, P. Tartaglia, and E. Zaccarelli, Langmuir **20**, 10 756 (2004).